Received: 8 December 2023 | Accepted: 29 July 2024

DOI: 10.1111/eve.14040

Equine Veterinary Education BEVA AAEP

CASE REPORT

Computed tomographic findings of a nasal neuroendocrine neoplasm with intracranial extension in a horse

Maria Elisabetta Giorio[1] | Jordan L. Mitchell[2] | Simon L. Priestnall[2] | Bettina Dunkel[1] | Rupert F. Dash[1] | Dagmar Berner[1]

[1]Department of Clinical Science and Services, Equine Referral Hospital, Royal Veterinary College, University of London, Hatfield, UK

[2]Department of Pathobiology and Population Sciences, Royal Veterinary College, Hatfield, UK

Correspondence: Maria Elisabetta Giorio
Email: mgiorio22@rvc.ac.uk

Summary

A 20-year-old Irish Sport Horse gelding was presented to the Royal Veterinary College Equine Referral Hospital for investigation of left-sided epistaxis, depression and gait abnormalities of approximately 1 month duration. Physical examination and cranial nerve evaluation were unremarkable. A small amount of haemorrhagic discharge was noted from the left nostril. Gait evaluation was suggestive of proprioceptive deficits. Computed tomography (CT) identified a mass lesion within the left conchofrontal and sphenopalatine sinuses extending through the cribriform plate into the calvarium. Histopathology of the mass revealed a neuroendocrine neoplasm, for which a diagnosis of esthesioneuroblastoma was favoured. This case highlights the usefulness of CT for the identification and extent of an intracranial mass and therefore its prognosis, however, histopathological examination was necessary to confirm the diagnosis.

KEYWORDS
horse, CT, esthesioneuroblastoma, head, neoplasia

INTRODUCTION

Neoplastic mass lesions within the nasal and paranasal cavities are a relatively uncommon finding in horses, representing between 2% and 19% of all sinonasal disorders (Boulton, 1985; Tremaine & Dixon, 2001a, 2001b). Differentiation of sinonasal neoplasia from non-neoplastic lesions, such as paranasal sinus cysts, ethmoid hematomas or nasal polyps, is of vital importance to allow the formulation of an appropriate treatment plan and to inform prognosis. Cross-sectional imaging, and in particular, computed tomography (CT), is a useful tool for identification and assessment of disorders affecting the equine nasal and paranasal sinus systems. Having the advantage of excellent contrast and spatial resolution, without anatomical superimposition, CT provides greater information than radiography regarding the extent of a mass lesion and features of malignancy (Cissell et al., 2012).

Neuroendocrine neoplasms of the respiratory tract are relatively rare and arise from either epithelial (neuroendocrine carcinoma) or neuroectodermal (esthesioneuroblastoma [olfactory neuroblastoma]) cells (Klöppel, 2017; Martí-García et al., 2023; Shah & Perez-Ordóñez, 2016). A small number of cases of nasal neuroendocrine neoplasia in horses has been reported, which describe their histopathological features (Döpke et al., 2005; Yamate et al., 2006) and their CT characteristics (Cissell et al., 2012; Tucker et al., 2016).

This report comprehensively illustrates the clinical presentation, CT and histopathological features of a case of neuroendocrine neoplasia with cribriform bone involvement and intracranial extra-axial extension in a 20-year-old horse. In this case, the use of standing CT proved to be of essential diagnostic and prognostic values.

CASE HISTORY

A 20-year-old Irish Sport Horse gelding was presented to the Royal Veterinary College Equine Referral Hospital for investigation of left-sided epistaxis, depression and gait abnormalities of approximately one month duration.

CLINICAL FINDINGS

Upon presentation, the gelding was quiet and subdued but responsive to stimulation. The horse was over-conditioned, with a body condition score of 7/9 (Henneke et al., 1983). Physical examination and cranial nerve evaluation were unremarkable. A small amount of haemorrhagic discharge was noted from the left nostril. A standing tail pull was suggestive of weakness. Gait evaluation identified occasional stumbling and poor coordination in all four limbs, suggestive of proprioceptive deficits or generalised weakness. When walking in a straight line, the gelding drifted to the left. Blindfolding resulted in more pronounced placement deficits and drifting to the right. Based on the neurological examination, namely changes in mentation, hypo-responsiveness, weakness and a tendency to drift to one side (interpreted as large-diameter circling), forebrain disease was considered most likely but a more diffuse disease process affecting brain and spinal cord could not be ruled out. The change in direction of the circling when blindfolded was unexpected and difficult to explain in conjunction with the other signs.

DIAGNOSIS

In accordance with the clinical signs, a lesion affecting the brain and sinuses was suspected, therefore, the gelding underwent CT examination of the head. An intravenous catheter was placed in the left jugular vein and following premedication with acepromazine (0.02 mg/kg bwt i.v., Dechra), sedation was administered to effect, using a combination of romifidine (0.05 mg/kg bwt i.v., Dechra) and methadone (0.1 mg/kg bwt i.v.). The CT examination was performed with the horse standing, using a 16-slice multidetector CT scanner, 120 kV, 400 mA and a 65 cm variable field of view (GE Medical Systems, LightSpeed RT 16). Images were reconstructed in a bone window (slice thickness 0.6 mm, interslice interval 0.3 mm, WW: 2800, WL: 800, bone kernel), soft tissue window (slice thickness 3.75 mm, interslice interval 1.5 mm, WW: 350, WL: 80, soft tissue kernel) and brain window (slice thickness 5 mm and interslice interval 2.5 mm, WW: 100, WL: 50, soft tissue kernel) in a 512 × 512 matrix. Images were viewed using a DICOM viewer (OsiriX, Pixmeo SARL) and multiplanar and three-dimensional reconstructions. A board-certified European College of Veterinary Diagnostic Imaging (ECVDI) diplomate and a third-year ECVDI resident reviewed the study.

Within the left conchofrontal and sphenopalatine sinuses, a large (78 × 99 × 53 mm, rostrocaudal × dorsoventral × lateromedial), heterogenous, irregularly marginated, soft tissue attenuating structure was identified. The Hounsfield units (HU) of this structure measured a mean of 40 HU, ranging from −10 to 55 HU. This structure was abutting the nasal septum and the frontal bone at the medial aspect of the orbit, where there was mild bone thickening and irregular periosteal bone formation. This structure was exerting a mass effect, causing expansion and loss of the normal structure of the ethmoidal turbinates and sinus. This lesion was continuous with a moderate-sized (28 × 34 mm, lateromedial × dorsoventral) round geographic region of bone loss in the rostrodorsal aspect of the left half of the calvarium and cribriform plate (Figure 1). In the region of the rostral aspect of the left olfactory and frontal lobes of the brain, there was a focal, ill-defined, oval-shaped and mildly heterogeneous area of mildly increased attenuation with slightly undulating margins. Adjacent to this and extending caudoaxially to it, a large relatively well-defined rim of hypoattenuation was noted within the left frontal lobe, which resembled the shape of the white matter tracts. Together this was causing left-to-right midline shift and mild displacement and compression of the lateral ventricles (Figure 2). The right medial retropharyngeal lymph node was mildly enlarged. An intravenous contrast (IVC) study was not performed for financial reasons.

In conclusion, CT of the head identified an expansile soft tissue mass rostral and caudal to the cribriform plate. This was causing bone lysis and periosteal reaction, suggestive of an aggressive lesion with an intra-cranial, extra-axial component. These findings were deemed to most likely represent a neoplastic mass which had invaded the calvarium (differential diagnosis: neuroendocrine tumour, adenocarcinoma, squamous cell carcinoma). The hypoattenuating rim within the left frontal lobe likely represented perilesional, cerebral oedema.

The neurological abnormalities corresponded largely with a predominately left-sided forebrain lesion while the epistaxis was likely caused by the soft tissue mass affecting the cribriform plate.

OUTCOME

The CT findings were discussed with the owner and the gelding was euthanased due to the grave prognosis. A post-mortem examination was subsequently performed.

POST-MORTEM FINDINGS

Gross examination identified an approximately 75 × 110 × 50 mm (rostrocaudal × dorsoventral × lateromedial) unilateral neoplasm within the caudal nasal cavity, with lysis of the cribriform plate and extension and invasion into the calvarium (Figure 3). There was displacement of the ethmoid turbinates and periosteal reaction of the frontal bone overlying the mass. The brain was removed from the cranium with difficulty, suggesting local adherence and compression, or possible invasion of the left olfactory bulb. There was no gross evidence of metastatic disease in the thoracic or abdominal viscera or cavities. These findings

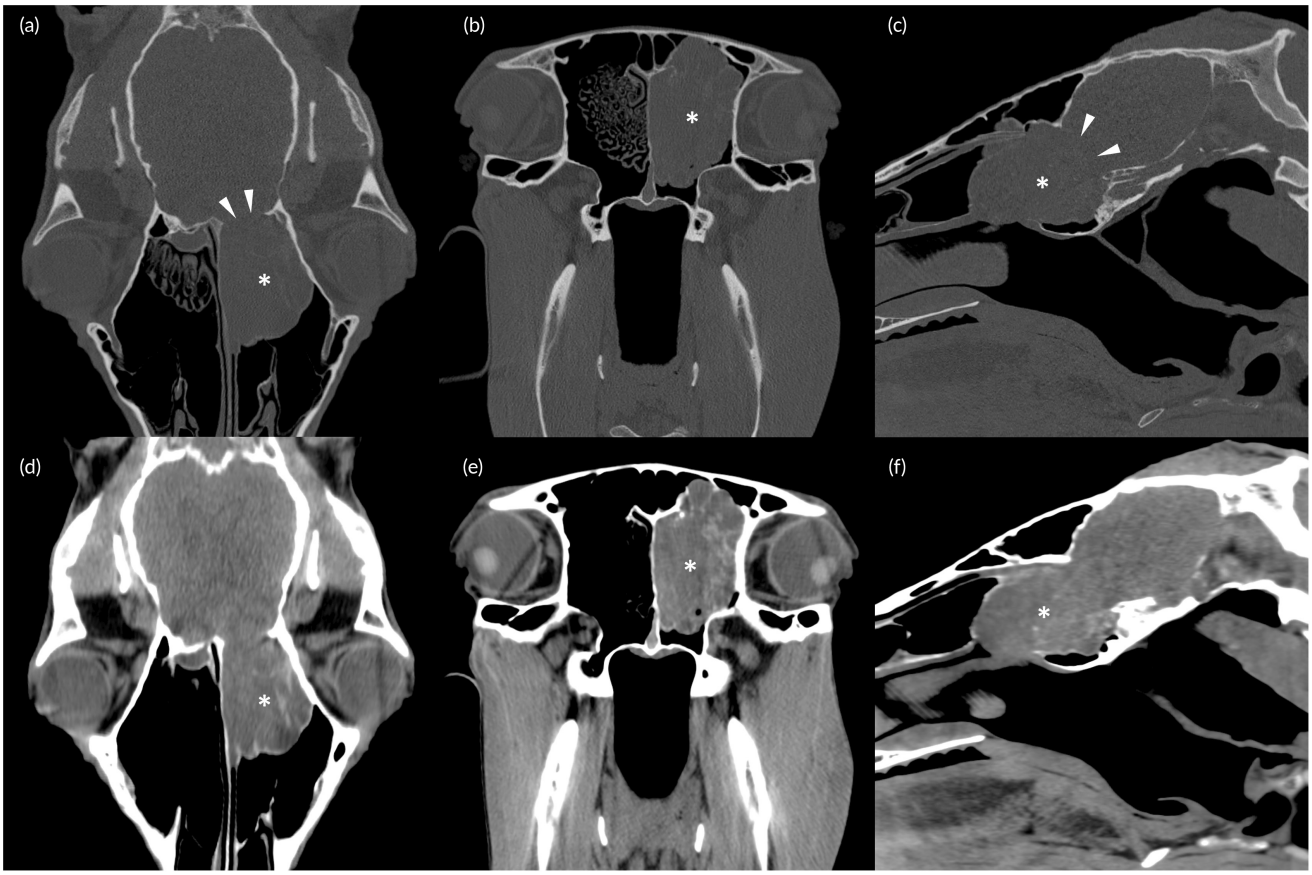

FIGURE 1 Dorsal (a, d), transverse (b, e) and sagittal (c, f) multiplanar reconstruction CT images in a bone (a–c) and soft tissue window (d–f). Within the left conchofrontal and the left sphenopalatine sinuses a large (78 × 99 × 53 mm, rostrocaudal × dorsoventral × lateromedial), markedly heterogenous, irregularly marginated, soft tissue attenuating structure was identified. This was exerting a mass effect, causing expansion and loss of the normal structure of the ethmoidal turbinates and sinus and was continuous with a large (28 × 34 mm, lateromedial × dorsoventral) round defect in the rostrodorsal aspect of the left half of the calvarium and cribriform plate.

were consistent with an expansile malignancy originating from the nasal cavity with cribriform plate lysis and intracranial invasion.

Histopathological examination confirmed the nasal mass as a moderately cellular, well-demarcated, nodular, expansile, encapsulated malignant neoplasm (Figure 4). Neoplastic cells were divided into loosely packed lobules of varying size by broad, anastomosing collagenous septa, which ranged from thin and fibrillar to thick and extensive. Neoplastic cells often showed a palisading pattern around the edge of lobules, and there were infrequent rudimentary rosettes. Neoplastic cells were round to polygonal and in places were slightly spindloid in morphology, with variably distinct cell borders, and a scant to a small amount of granular, eosinophilic cytoplasm, a single, often centrally located nucleus with finely stippled chromatin and, where visible, one to two nucleoli. There was moderate anisocytosis and anisokaryosis. There were 34 mitotic figures across 10 high-power fields (2.37 mm^2), with rare, bizarre mitoses. At the centre of larger lobules of neoplastic cells focal areas of coagulative and lytic necrosis were present, with admixed haemorrhage and infiltration with neutrophils and foamy macrophages. Remodelling of sinus and turbinate bone within and surrounding the tumour was evident, with pre-existing bone lined by plump, reactive osteoblasts, and there were multifocal areas of new bone formation and bone lysis. Multifocally throughout the neoplasm were entrapped nerves, and in the caudal aspect of the neoplasm, there was direct apposition of the fibrous capsule of the neoplasm and meninges with the underlying neuroparenchyma, indicating effacement and loss of the cribriform plate. There were multifocal peritumoral infiltrates of moderate numbers of lymphocytes and plasma cells, in addition to multifocal mild meningeal lymphoplasmacytic infiltration. The superficial grey matter of the left frontal lobe exhibited mild, multifocal rarefaction and pallor. These findings were consistent with a neuroendocrine neoplasm, for which a diagnosis of esthesioneuroblastoma (olfactory neuroblastoma) was favoured, but neuroendocrine carcinoma could not be excluded. Immunohistochemistry or electron microscopy to differentiate between these two neoplasms was not performed for financial reasons.

DISCUSSION

Clinical implications

While unilateral epistaxis was suggestive of nasal or sinus disease, the subdued mentation, weakness and possible wide circling indicated an intracranial, likely fore-brain lesion. Blind-folding during

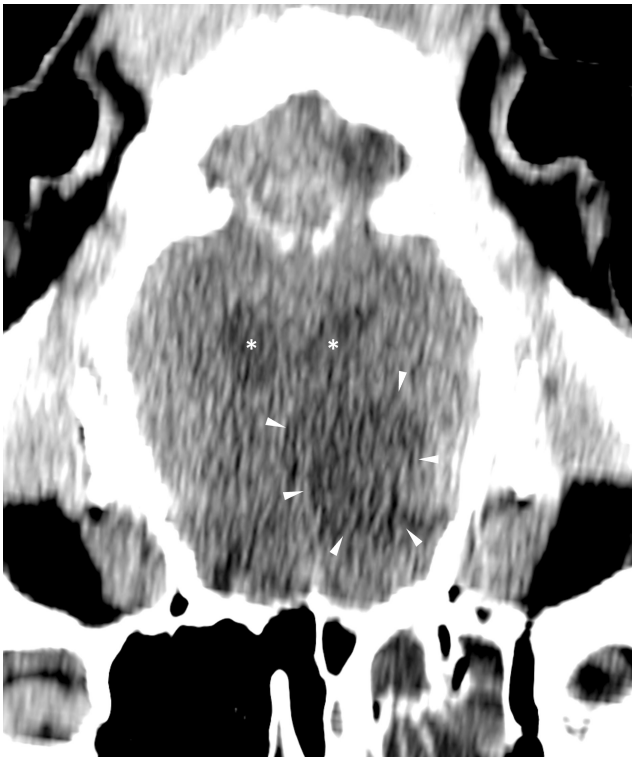

FIGURE 2 Dorsal multiplanar reconstruction computed tomography image in a brain window showing a large relatively well-defined area of hypoattenuation within the left frontal lobe, resembling the shape of the white matter tracts (arrow heads). This was causing mild right shift and compression of the lateral ventricles of the brain (asterisks).

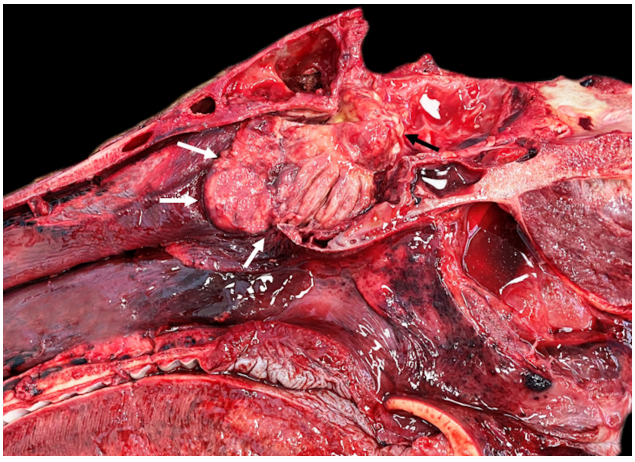

FIGURE 3 Sagittal section through the skull. In the caudal nasal cavity arising from the ethmoid turbinates is a locally infiltrative, multilobulated, firm, cream mass (white arrows) which extends into the cranial vault (black arrow, brain removed).

a neurological assessment is a useful tool to identify chronic vestibular disease or to exacerbate subtle neurological deficits (Olsen et al., 2014). The reason for the change in direction of the wide circling when blind-folded was unexpected and has, to the authors' knowledge, not been described as a feature of forebrain or other neurological disease in horses. Severe sinus disease can lead to a quiet or subdued mentation, but true neurological deficits as seen in this case are highly unusual. Other signs suggesting sinus disease such as unilateral nasal discharge or distortion of the facial contours, as seen in more chronic cases, were absent. The change in mentation, weakness and possible circling suggested intracranial, forebrain, disease, which is rarely associated with epistaxis. A thrombocytopaenia, platelet dysfunction or coagulopathy secondary to meningitis or intracranial mass would be possible but should present as bilateral epistaxis. An invasive process, affecting the sinus or nasal cavity with extension into the brain was therefore suspected.

Technical considerations: The use of cross-sectional imaging and IV contrast administration

Endoscopy only offers a limited assessment of the area, and head radiographs have low to moderate sensitivity for identification of sinonasal disease (Manso-Díaz, Garcia-Lopez, et al., 2015) due to superimposition of bony structures (Barrett & Easley, 2013), a CT offered the best chance of achieving a fast and accurate diagnosis. Either CT or magnetic resonance imaging (MRI) can be used to achieve a detailed examination of the equine head (Manso-Díaz, Dyson, et al., 2015). MRI is superior to CT for soft tissue depiction and is considered the gold-standard cross-sectional imaging modality for studying the equine brain as well as extracranial soft tissues and space-occupying lesions in the nasal and paranasal sinus system (Matiasek et al., 2007; Manso-Díaz et al., 2021). Conversely, CT is superior for the evaluation of small bone details including the presence of bone lysis and periosteal reaction. Currently, MRI of the equine head can only be carried out under general anaesthesia, with increased costs and risks compared to a standing procedure such as CT.

Intravenous contrast (IVC) media administration can help accurately locate, depict the margination and characterise soft tissue masses, providing increased attenuation in (neo)vascularised structures compared with the native CT images (Crijns et al., 2016). Alteration of contrast enhancement within tumoural tissues is caused by the process of angiogenesis, which increases perfusion and capillary permeability, promoting tumour growth and metastasis (Miles, 1999). In a recent study, 13 of 15 sinonasal tumours were difficult to distinguish from the adjacent tissues due to similar attenuation and IVC administered in two horses resulted in significant increased intralesional attenuation (Cissell et al., 2012). However, the use of IVC in the standing horse is challenging. In fact, a large volume of contrast medium (200–600 mg of iodinated contrast/kg bodyweight [Carmalt & Montgomery, 2015; Manso-Díaz et al., 2021]) is required which considerably increases the cost of the procedure. Its administration must be fast; therefore, placement of bilateral large-bore intravenous jugular catheters is necessary, increasing the risk of catheter complications. Following administration, a short window of time is available for image acquisition and should the horse move during this time the study will be non-diagnostic. The

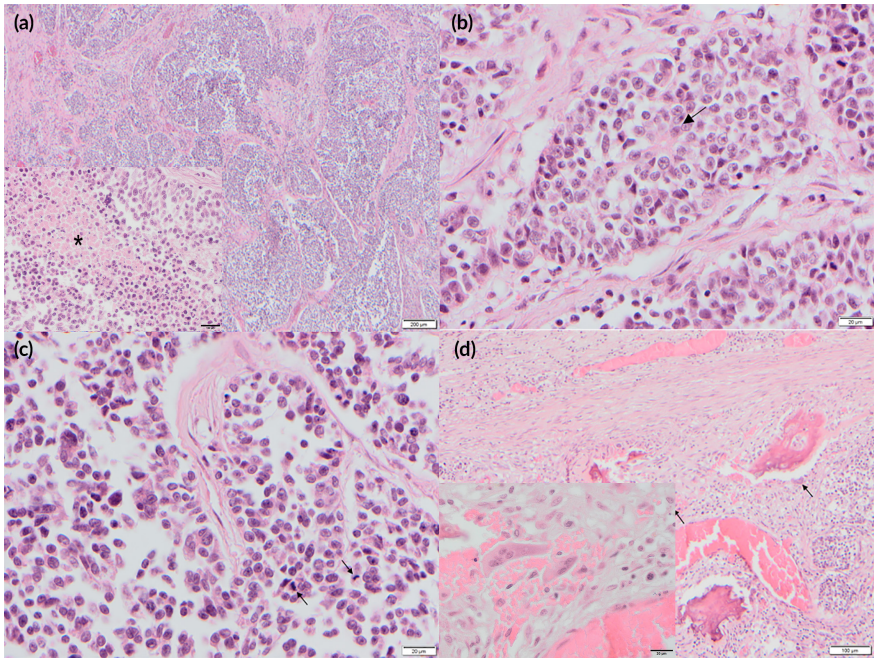

FIGURE 4 Histopathological features of the tumour, consistent with a neuroendocrine/neuroepithelial origin. Haematoxylin–eosin. (a) Subgross examination identifies a moderately cellular neoplasm divided into lobules by broad, anastomosing collagenous septa. ×4 objective. Multifocally, within the centre of large lobules of neoplastic cells are areas of necrosis (inset, black asterisk). ×20 objective. (b) Neoplastic cells infrequently form rosettes (black arrow). ×40 objective. (c) Neoplastic cells are artefactually individualised due to autolysis and exhibit moderate anisocytosis and anisokaryosis, with frequent mitotic figures (black arrows). ×40 objective. (d) There is active bone remodelling associated with the tumour and moderate numbers of osteoclasts (black arrows). ×20 objective. Insert demonstrating multinucleated osteoclasts associated with the tumour. ×40 objective.

use of intraarterial contrast in horses under general anaesthesia, leads to similar contrast enhancement with a smaller dose of contrast medium compared to the intravenous technique (Carmalt & Montgomery, 2015; Crijns et al., 2016). However, the applicability of this technique in standing horses has not been reported. Therefore, considering that in this case, the extent of the lesion was already appreciable on unenhanced images, the cost implication and the potential risks of seizures, the use of contrast was declined.

Imaging features and DDx

Computed tomography showed a heterogeneous soft tissue mass, expanding from the cribriform plate and causing bone lysis and periosteal reaction. Sinonasal neoplasia and non-neoplastic diseases in horses can have similar imaging features and the use of CT can help to differentiate between the two. In a recent study, perforation of the cribriform plate, calvarium or orbit seen on CT was always associated with malignancy (Tucker et al., 2016). Similarly, Cissell et al. (2012) reported that neuroendocrine/neuroblastoma originates consistently from the retrobulbar space or from the ethmoid turbinates and they show cribriform bone involvement with intracranial extension. However, several other mass lesions have similar CT appearance, including carcinomas and sarcomas, as well as benign neoplasms such as myxoma and ossifying fibromas (Cissell et al., 2012). Neoplasia of epithelial origin (squamous cell carcinoma and adenocarcinoma) has been reported as the most common pathological process involving the sphenopalatine sinus (Tucker et al., 2016). Squamous cell carcinomas are the most common nasal and paranasal tumours in horses and cause mild to severe, solid periosteal reaction and cortical lysis as well as frequent concurrent enlargement of the mandibular and retropharyngeal lymph nodes (Strohmayer et al., 2020). However, lymphomas can have similar MRI features to those of squamous cell carcinoma (Manso-Díaz, Dyson, et al., 2015). Adenocarcinomas are highly infiltrative masses, originating from the glands overlying the ethmoid turbinates and extending through the cribriform plate into the periorbital region and the olfactory bulb (Manso-Díaz, Dyson, et al., 2015). Bone disruption secondary to an expansile mass lesion in the equine sinonasal system is also a common feature of three reported cases of sarcoma (Veraa et al., 2009). Ossifying fibromas generally differ from other tumour types by their diffuse, hyperattenuating opacity and extensive mineralisation, but this can vary widely depending on the degree of ossification present in different cases (Cissell et al., 2012). Equine sinonasal myxomas are very rare, benign neoplasms, that show mild intralesional mineralisation and ethmoidal localisation with mild cortical bone lysis.

Although bone involvement is a common feature of sinonasal tumours (Cissell et al., 2012), this cannot be considered a pathognomonic sign as other expansile masses, such as progressive ethmoid hematomas (PEH) or paranasal sinus cysts (PSC), can cause pressure necrosis of the surrounding bone and interruption of the cribriform plate (Frees et al., 2001; Ostrowska et al., 2020; Tremaine, 2013).

However, in contrast to the relatively homogenous appearance and presence of bone reaction of most tumours described by Cissell et al. (2012), PEH show a characteristic mixed, hyperattenuating swirling pattern and do not cause periosteal reaction (Textor et al., 2012). Paranasal sinus cysts show a typical homogeneous internal attenuation with a hyperattenuating mineralised wall, in contrast with the heterogenous appearance of the lesion described in the current study, and often cause new bone formation, but this is only focal and mild (Ostrowska et al., 2020).

Prognostic information

Standing CT was able to identify the presence, location, and extent of the lesion, providing invaluable prognostic information. Based on the invasive nature of the mass extending through the cribriform plate into the calvarium, the mass was considered not operable and clinical signs were therefore non-reversible and likely progressive. This guided the management and clinical outcome. Forebrain disease can be associated with seizures and therefore represents a significant risk to the horse and horse owner and handlers. The poor long-term prognosis and health risks associated with progressive neurological disease contributed to the decision for euthanasia.

Post-mortem diagnosis

Considering that CT alone cannot categorically determine the nature of soft tissue masses in the nasal and paranasal sinus systems (Cissell et al., 2012; Tucker et al., 2016), histopathology was necessary to reach a definitive diagnosis in this case. Microscopic examination identified a neuroendocrine tumour but differentiation between esthesioneuroblastoma and neuroendocrine carcinoma is challenging due to the overlap of histopathological features of these tumour types, and arguably these two tumours may represent different manifestations of the same entity. The presence and frequency of rosettes are more indicative of esthesioneuroblastoma, although ultrastructural examination is required to provide a more conclusive diagnosis. These are rare malignancies in veterinary species, arising from precursor cells of the nasal neuroepithelium. In a previous report on this tumour in a horse (Döpke et al., 2005), an extensive tumour involving the left ethmoid bone, maxillary sinus, superior turbinate and orbit, resulting in proptosis, and microscopically tumour emboli were present in the choroid and there was focal infiltration of the retina by neoplastic cells. Both esthesioneuroblastoma and neuroendocrine carcinoma can be locally aggressive (van Maanen et al., 1996), as seen in this case with lysis of the cribriform plate and extension into the cranial vault.

Post-mortem examination showed good agreement with the CT findings in regard to the size and location of the mass lesion, as well as the presence of bone involvement, however, post-mortem examination was superior to CT for assessment of the precise extent and margination of the lesion. The heterogeneous appearance of the mass on CT correlated well with the presence of focal necrotic areas (hypoattenuating on CT) at the centre of larger lobules of neoplastic cells and bone remodelling (hyperattenuating on CT) within and surrounding the mass seen on histopathology. The intra-axial area of hypoattenuation surrounding and caudal to the mass lesion was likely consistent with secondary vasogenic cerebral oedema. Histopathological examination of the left frontal lobe identified mild, superficial rarefaction of the grey matter neuropil, but given the delay between euthanasia and post-mortem examination, the degree of fixation delay artefact and autolysis in the neuroparenchyma may obscure or mimic true cerebral oedema. On CT examination, the hypoattenuating area was relatively well defined and was following the white matter tracts, which is the typical appearance and distribution of vasogenic cerebral oedema (Zhang et al., 2022).

CONCLUSIONS

This report described the imaging features of an aggressive mass, centred on the cribriform plate which on histology was determined to be a nasal neuroendocrine tumour. The use of standing CT was of crucial importance in informing the nature of disease, the extent of forebrain involvement, and prognosis. The location of this mass is compatible with a neuroendocrine neoplasm but is not unique to this tumour type. Therefore, a definitive diagnosis could only be achieved by histology.

AUTHOR CONTRIBUTIONS

Maria Elisabetta Giorio: Conceptualization; writing – original draft; writing – review and editing; data curation; validation; project administration; supervision. **Jordan L. Mitchell:** Writing – original draft; writing – review and editing; data curation; conceptualization; validation; supervision. **Simon L. Priestnall:** Writing – review and editing; supervision; validation; data curation. **Bettina Dunkel:** Conceptualization; methodology; writing – review and editing; validation; supervision; data curation. **Rupert F. Dash:** Writing – review and editing; data curation; supervision; validation; writing – original draft. **Dagmar Berner:** Conceptualization; methodology; writing – review and editing; validation; supervision; data curation; project administration.

ACKNOWLEDGEMENTS

We would like to thank Dr Alejandro Suárez-Bonnet (Department of Pathobiology and Population Sciences, Royal Veterinary College) for assistance with images, and the post-mortem room and histopathology, equine diagnostic imaging technicians and all staff of the equine referral hospital for their assistance with this case.

FUNDING INFORMATION

There are no funders for this case report.

CONFLICT OF INTEREST STATEMENT

None declared.

ETHICS STATEMENT

Ethical approval was not required according to the policy of the Clinical Research Ethical Review Board at The Royal Veterinary College. Informed client consent for inclusion in the study was obtained.

ORCID

Maria Elisabetta Giorio https://orcid.org/0009-0006-6849-8345
Bettina Dunkel https://orcid.org/0000-0003-2041-2144
Rupert F. Dash https://orcid.org/0000-0003-4955-8841
Dagmar Berner https://orcid.org/0000-0001-6442-3449

REFERENCES

Barrett, M.R. & Easley, J.T. (2013) Acquisition and interpretation of radiographs of the equine skull. *Equine Veterinary Education*, 25, 643–652.

Boulton, C.H. (1985) Equine nasal cavity and paranasal sinus disease: a review of 85 cases. *Journal of Equine Veterinary Science*, 5, 5–275.

Carmalt, J.L. & Montgomery, J. (2015) Intraarterial injection of iodated contrast medium for contrast enhanced computed tomography of the equine head. *Veterinary Radiology and Ultrasound*, 56(4), 384–390.

Cissell, D.D., Wisner, E.R., Textor, J., Mohr, F.C., Scrivani, P.V. & Theon, A.P. (2012) Computed tomographic appearance of equine sinonasal neoplasia. *Veterinary Radiology and Ultrasound*, 53(3), 245–251.

Crijns, C.P., Baeumlin, Y., De Rycke, L., Broeckx, B.J.G., Vlaminck, L., Bergman, E.H.J. et al. (2016) Intra-arterial versus intra venous contrast-enhanced computed tomography of the equine head. *BMC Veterinary Research*, 12, 6.

Döpke, C., Gröne, A., Borstel, M.V., Oppen, T.V., Boéve, M.H. & Baumgärtner, W. (2005) Metastatic Esthesioneuroblastoma in a horse. *Journal of Comparative Pathology*, 132, 218–222.

Frees, K.E., Gaughan, E.M., Lillich, J.D., Cox, J., Gorondy, D., Nietfeld, J.C. et al. (2001) Severe complication after administration of formalin for treatment of progressive ethmoid haematoma in the horse. *Journal of the American Veterinary Medical Association*, 219, 950–952.

Henneke, D., Potter, G., Kreider, J. & Yeates, B. (1983) Relationship between condition score, physical measurements and body fat percentage in mares. *Equine Veterinary Journal*, 15, 371–372.

Klöppel, G. (2017) Neuroendocrine neoplasms: dichotomy, origin and classifications. *Visceral Medicine*, 33(5), 324–330.

Manso-Díaz, G., Dyson, S.J., Dennis, R., Garcia-Lopez, J.M., Biggi, M., Garcia-Real, I. et al. (2015) Magnetic resonance imaging characteristics of equine head disorders: 84 cases (2000–2013). *Veterinary Radiology and Ultrasound*, 56, 176–187.

Manso-Díaz, G., Garcia-Lopez, J.M., Maranda, L. & Taeymans, O. (2015) The role of head computed tomography in equine practice. *Equine Veterinary Education*, 27, 136–145.

Manso-Díaz, G., Taeymans, O., García-López, J.M. & Weller, R. (2021) Application and indications of magnetic resonance imaging and computed tomography of the equine head. *Equine Veterinary Education*, 33(1), 31–46.

Martí-García, B., Priestnall, S.L., Holmes, E. & Suárez-Bonnet, A. (2023) Olfactory neuroblastoma in a domestic cat and review of the literature. *Veterinary Clinical Pathology*, 52(3), 521–526.

Matiasek, K., Cronau, M., Schmahl, W. & Gerhards, H. (2007) Imaging features and decision making in retrobulbar and neuroendocrine tumours in horses. Case report and review of literature. *Journal of Veterinary Medicine. A, Physiology, Pathology, Clinical Medicine*, 54, 302–306.

Miles, K.A. (1999) Tumour angiogenesis and its relation to contrast enhancement on computed tomography: a review. *European Journal of Radiology*, 30, 198–205.

Olsen, E., Dunkel, B., Barker, W.H.J., Finding, E.J.T., Perkins, J.D., Witte, T.H. et al. (2014) Rater agreement on gait assessment during neurologic examination of horses. *Journal of Veterinary Internal Medicine*, 28(2), 630–638.

Ostrowska, J., Lindström, L., Tóth, T., Hansson, K., Uhlhorn, M. & Ley, C.J. (2020) Computed tomography characteristics of equine paranasal sinus cysts. *Equine Veterinary Journal*, 52, 538–546.

Shah, K. & Perez-Ordóñez, B. (2016) Neuroendocrine neoplasms of the sinonasal tract: neuroendocrine carcinomas and olfactory neuroblastoma. *Head and Neck Pathology*, 10(1), 85–94.

Strohmayer, C., Klang, A. & Kneiss, S. (2020) Computed tomographic and histopathological characteristics of 13 equine and feline oral and sinonasal squamous cell carcinomas. *Frontiers in Veterinary Science*, 7, 591437.

Textor, J.A., Puchalski, S.M., Affolter, V.K., MacDonald, M.H., Galuppo, L.D. & Wisner, E.R. (2012) Results of computed tomography in horses with ethmoid hematoma: 16 cases (1993-2005). *Journal of the American Veterinary Medical Association*, 240, 1338–1344.

Tremaine, W.H. (2013) Progressive ethmoidal haematoma. *Equine Veterinary Education*, 25(10), 508–510.

Tremaine, W.H. & Dixon, P.M. (2001a) A long-term study of 277 cases of equine sinonasal disease. Part 1: details of horses, historical, clinical and ancillary diagnostic findings. *Equine Veterinary Journal*, 33, 274–282.

Tremaine, W.H. & Dixon, P.M. (2001b) A long-term study of 277 cases of equine sinonasal disease. Part 2: treatments and results of treatments. *Equine Veterinary Journal*, 33, 283–289.

Tucker, R., Windley, Z.E., Abernethy, A.D., Witte, T.H., Fishe-Jackson, A.R., Turner, S. et al. (2016) Radiographic, computed tomographic and surgical anatomy of the equine sphenopalatine sinus in normal and diseased horses. *Equine Veterinary Journal*, 48, 578–584.

Van Maanen, C., Klein, W.R., Dik, K.J., Van Den Ingh, T.S.G.A.M (1996) Three cases of carcinoid in the equine nasal cavity and maxillary sinuses: Histologic and immunohistochenical features. *Veterinary Pathology*, 33, 92–95.

Veraa, S., Dijkman, R., Klein, W.R. & van den Belt, J.M. (2009) Computed tomography in the diagnosis of malignant tumours in three horses. *Equine Veterinary Education*, 21(6), 284–288.

Yamate, J., Izawa, T., Ogata, K., Kobaiashi, O., Okajima, R., Kuwamura, M. et al. (2006) Olfactory neuroblastoma in a horse. *Journal of Veterinary Medical Science*, 68(5), 495–498.

Zhang, X., Huang, P. & Zhang, R. (2022) Post-stroke cerebral oedema based on neuroimaging. *Frontiers in Neurology*, 12, 763018.

How to cite this article: Giorio, M.E., Mitchell, J.L., Priestnall, S.L., Dunkel, B., Dash, R.F. & Berner, D. (2024) Computed tomographic findings of a nasal neuroendocrine neoplasm with intracranial extension in a horse. *Equine Veterinary Education*, 00, 1–7. Available from: https://doi.org/10.1111/eve.14040